Supporting Information

Promoting Polysulfide Redox Kinetics by Tuning Non-metallic *p*-Band of Mo-based compounds

Yajing Liu,[a,b,†] Jie Xu,[b,†] Yongjie Cao,[b] Mingqi Chen,[c] Nan Wang,[b] Donghui Long,[c] Yonggang Wang,[b] Yongyao Xia,[b*]

[a] College of Chemistry and Chemical Engineering, Qinghai Normal University, Xining, 810016, China

[b] Department of Chemistry and Shanghai Key Laboratory of Molecular Catalysis and Innovative Materials, Institute of New Energy, iChEM (Collaborative Innovation Center of Chemistry for Energy Materials), Fudan University, Shanghai 200433, China

[c] State Key Laboratory of Chemical Engineering, East China University of Science and Technology, Shanghai 200237, China

*E-mail: yyxia@fudan.edu.cn

[†] Y.L. and J.X. contributed equally to this work.

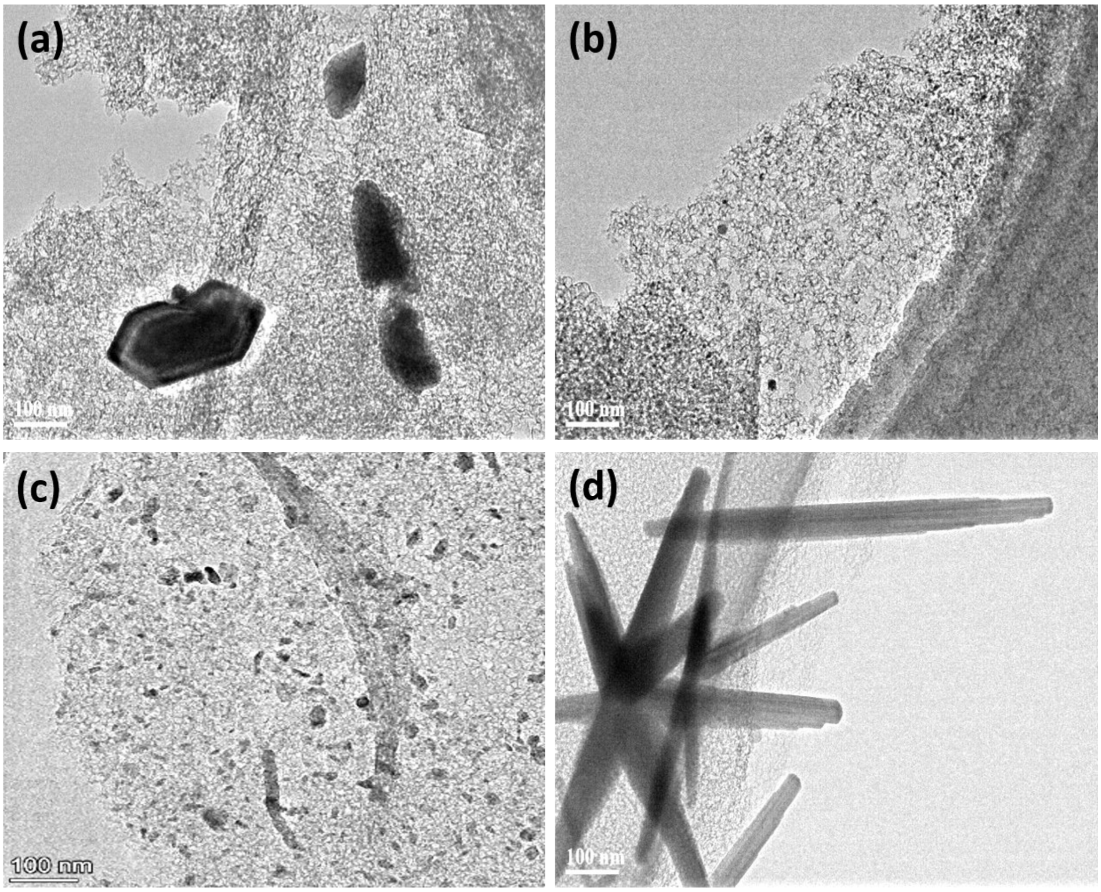

Fig. S1. (a-d) The TEM images of MCNs-MoO_2, MCNs-MoS_2, MCNs-MoN and MCNs-MoP, respectively.

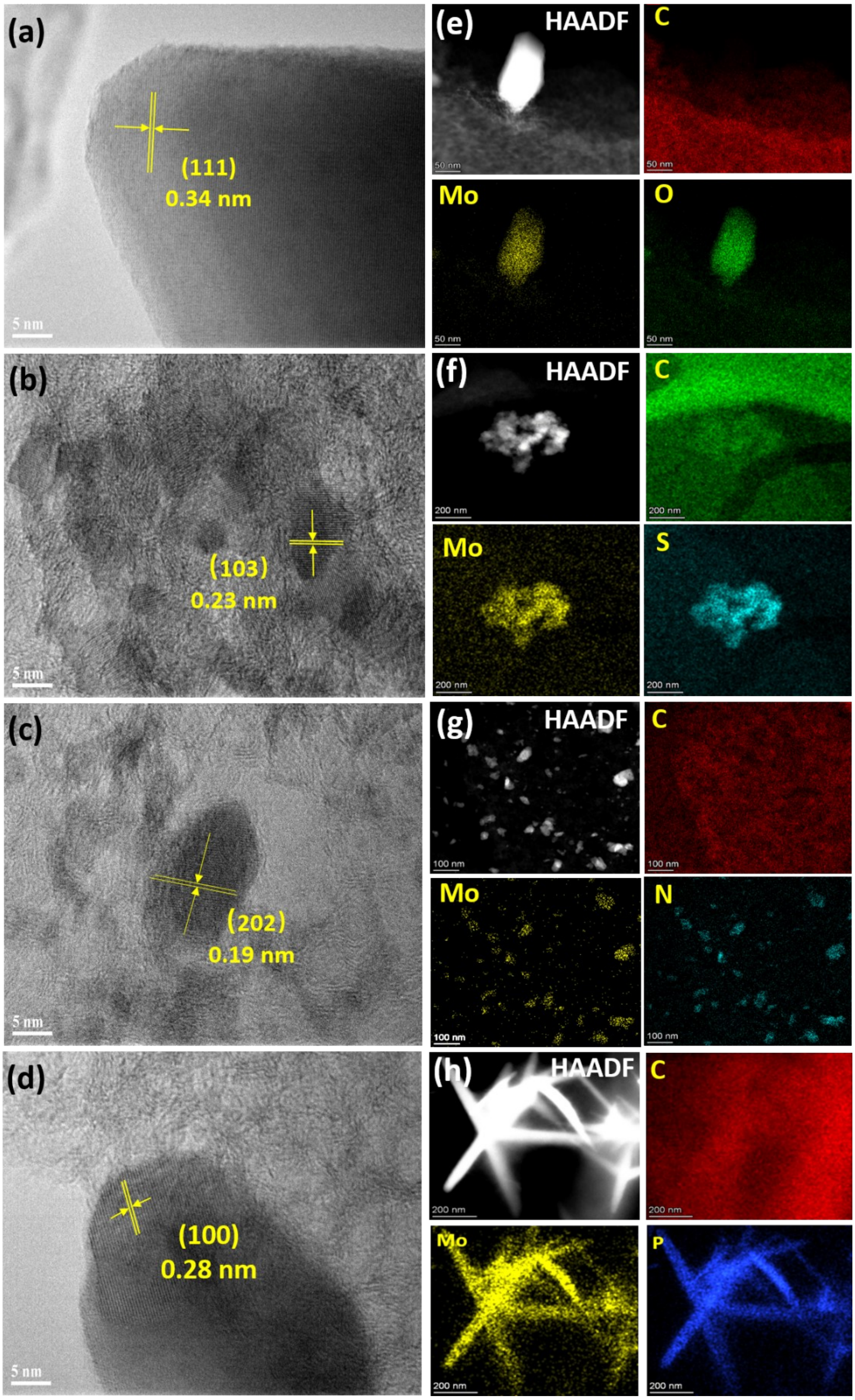

Fig. S2. (a-d) The HRTEM images of MCNs-MoO_2, MCNs-MoS_2, MCNs-MoN and MCNs-MoP. (e-h) The corresponding elemental mapping images.

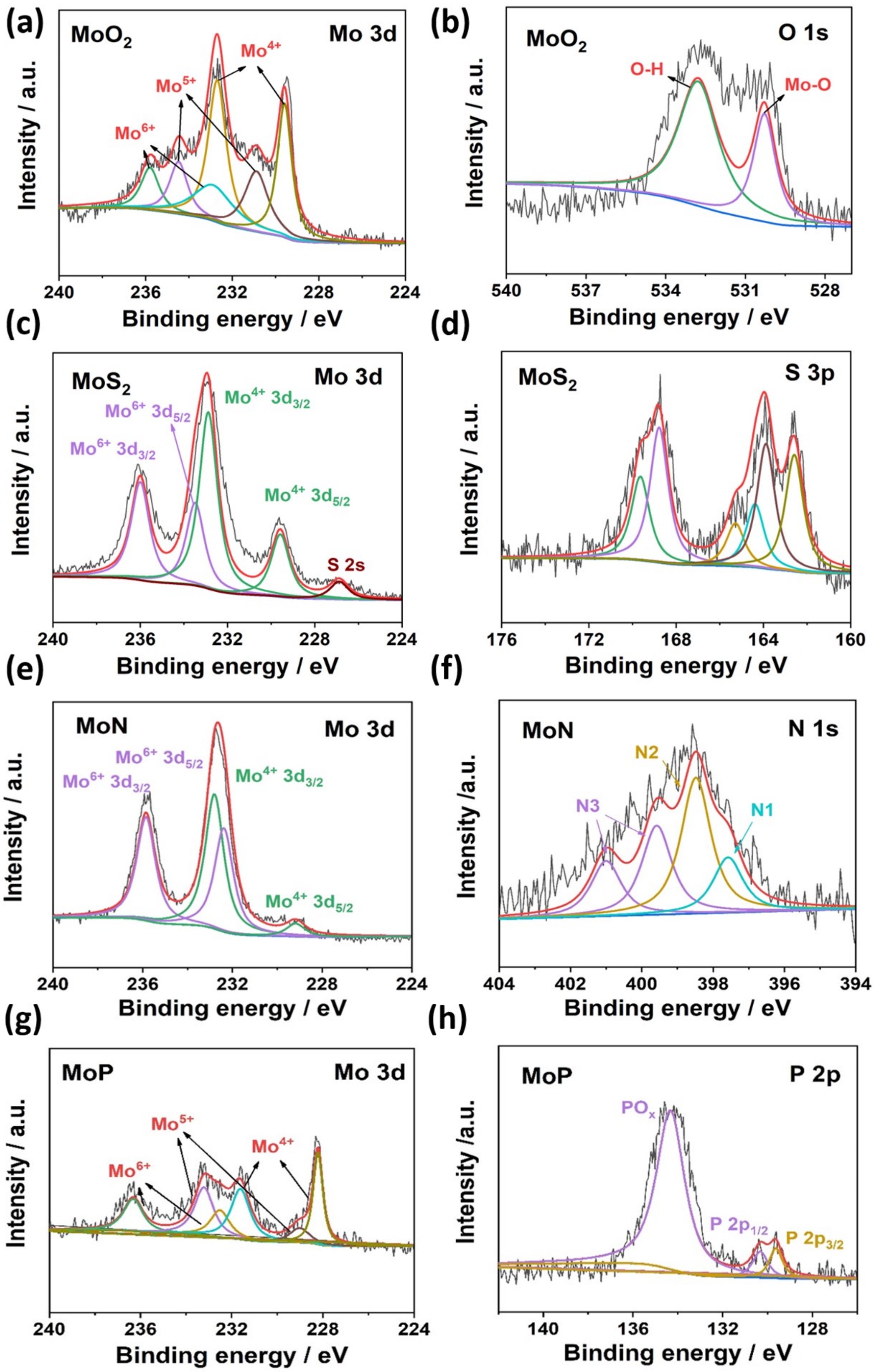

Fig. S3. The XPS core-level spectra of the prepared MCNs-Mo-based compounds.

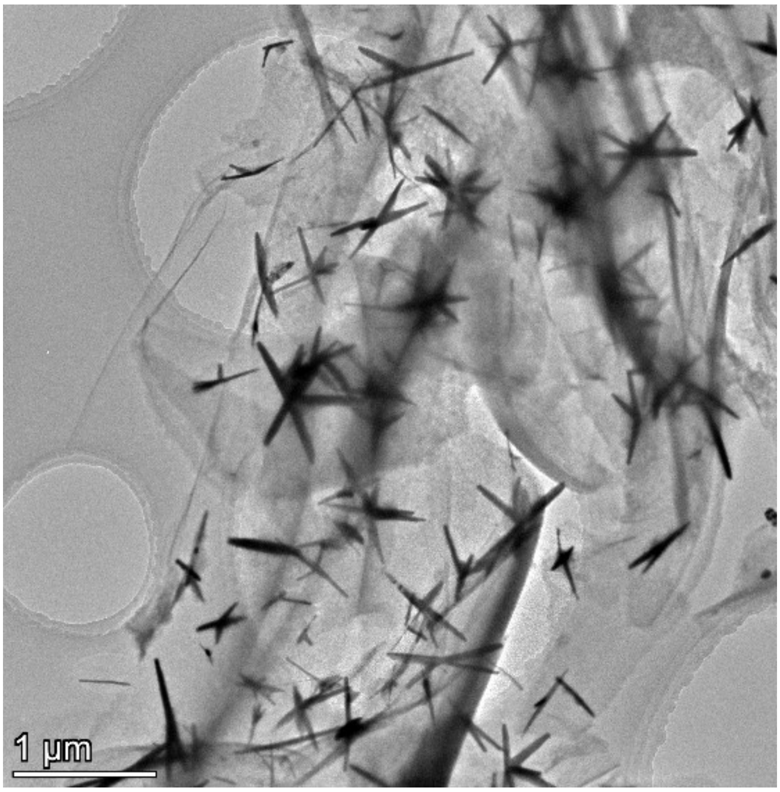

Fig. S4. The TEM images of MCNs-MoP.

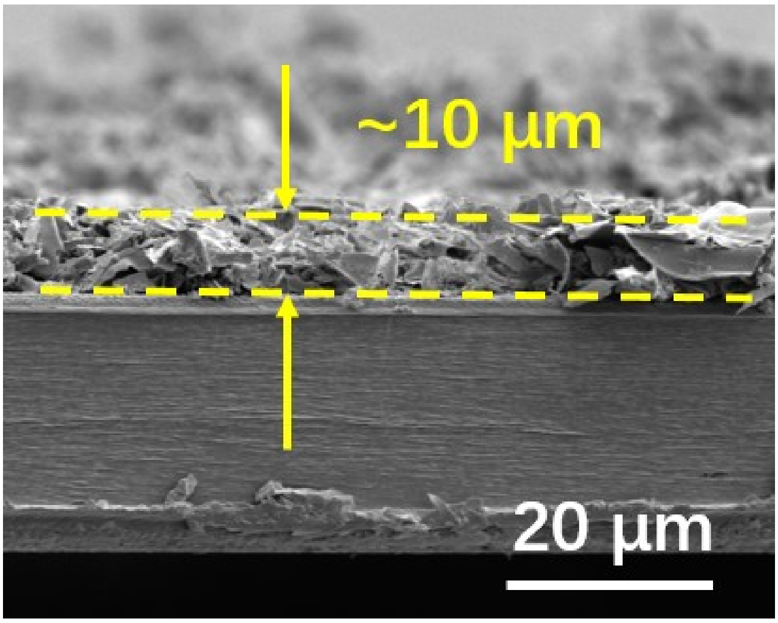

Fig. S5. Cross-sectional SEM image of MCNs-MoP separator.

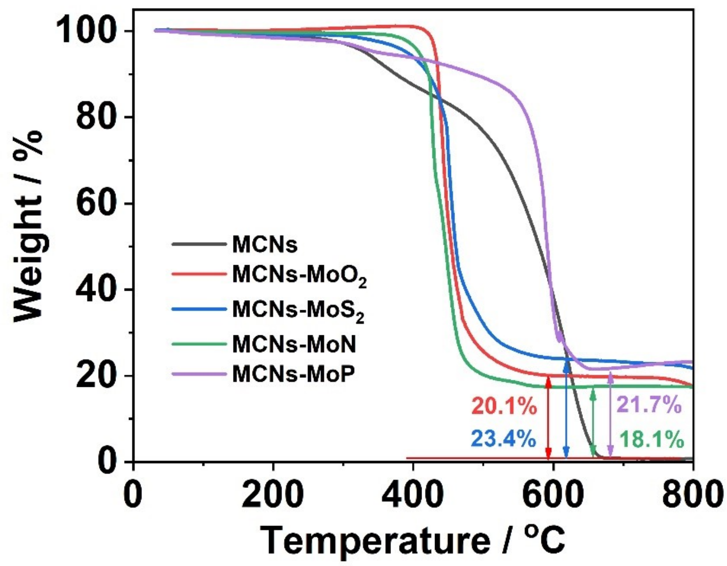

Fig. S6. TG profile of the MCNs, MCNs-MoO_2, MCNs-MoS_2 , MCNs-MoN, and MCNs-MoP in air atomosphere.

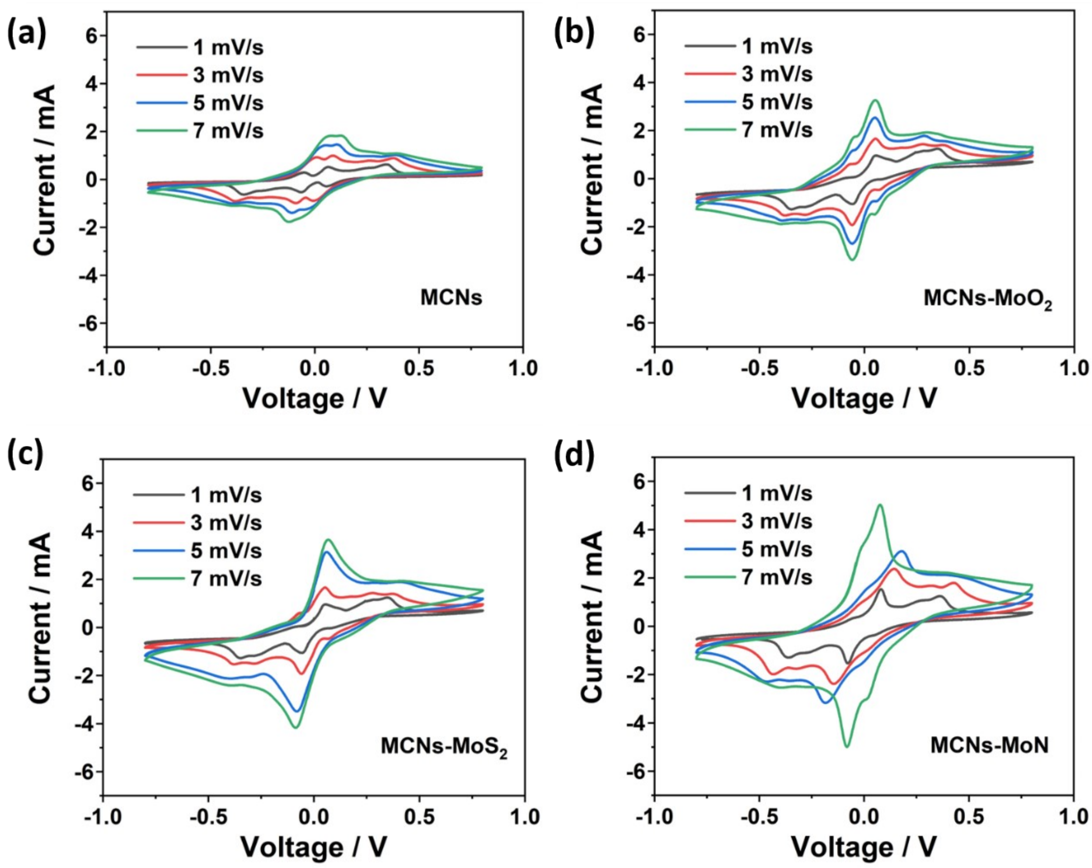

Fig. S7. The CV curves of **(a)** MCNs, **(b)** MCNs-MoO_2, **(c)** MCNs-MoS_2 and **(d)** MCNs-MoN in symmetric cells with different scan rates.

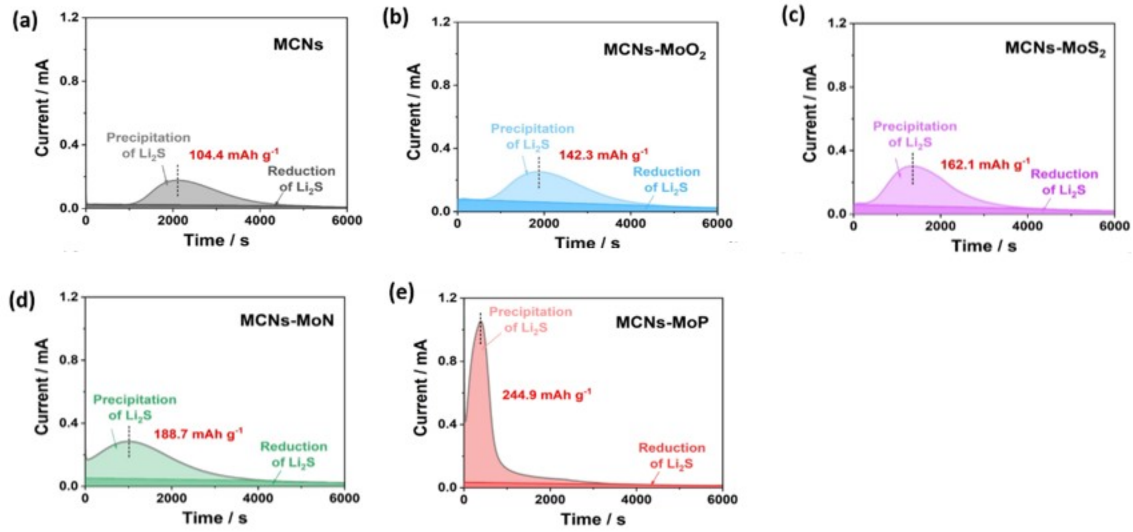

Fig. S8. Potentiostatic discharge of Li_2S_6 electrolyte on (a) MCNs, (b) MCNs-MoO_2, (c) MCNs-MoS_2, (d) MCNs-MoN_2 and (e) MCNs-MoP electrodes at 2.05 V. The dark and light colors indicate the reduction of Li_2S_6 and the precipitation of Li_2S, respectively.

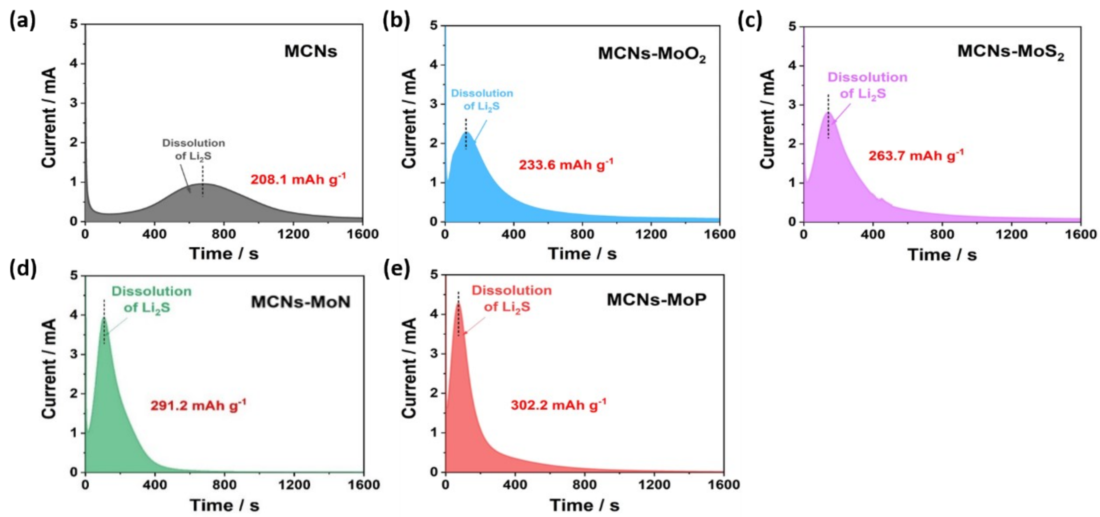

Fig. S9. Potentiostatic charge profiles at 2.40 V on (a) MCNs, (b) MCNs-MoO_2, (c) MCNs-MoS_2, (d) MCNs-MoN_2 and (e) MCNs-MoP electrodes to evaluate dissolution behaviors of Li_2S.

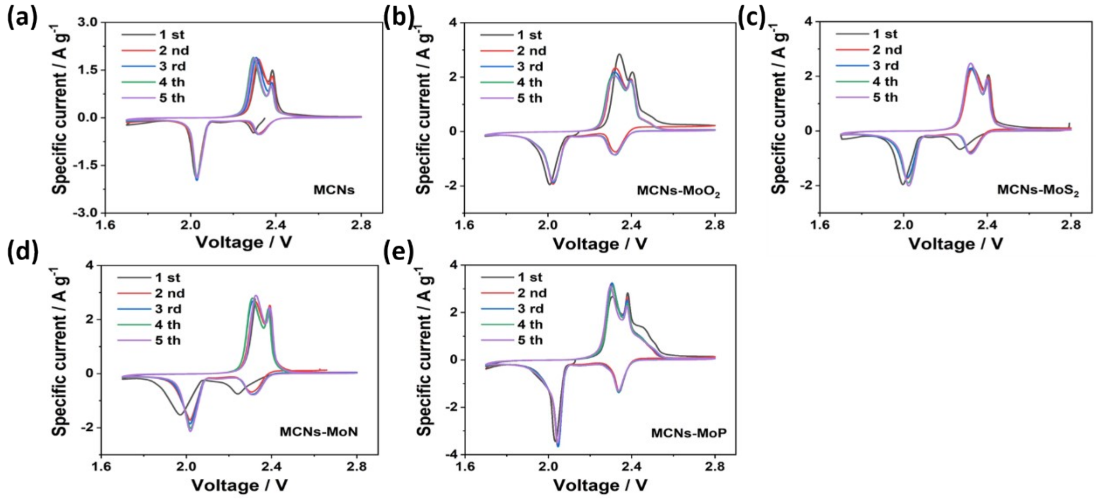

Fig. S10. (a-e) CV profiles of MCNs, MCNs-MoO_2, MCNs-MoS_2, MCNs-MoN_2 and MCNs-MoP configuration at a scan rate of 0.1 mV s^{-1} in first five cycles.

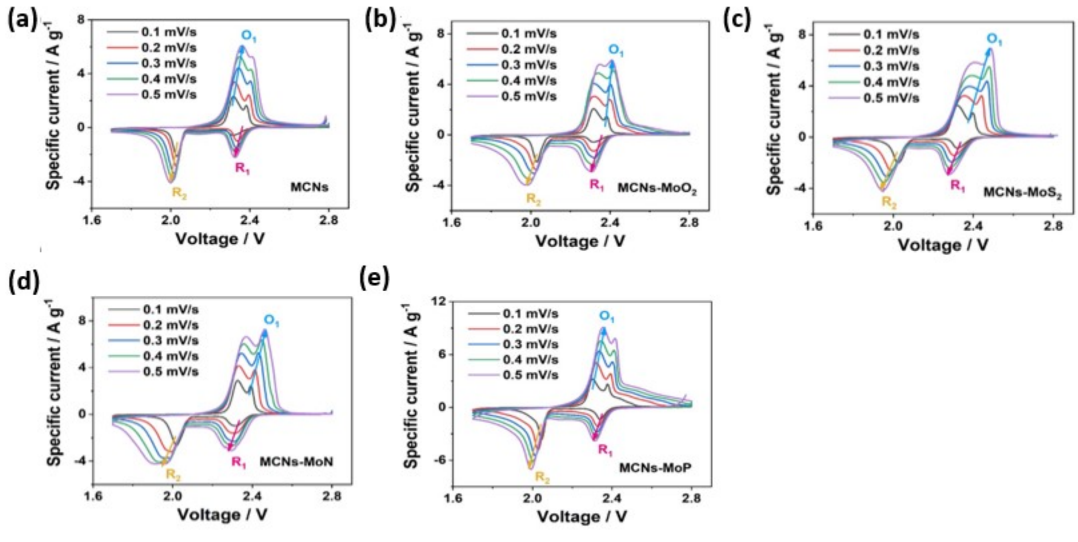

Fig. S11. (a-e) CV profiles of MCNs, MCNs-MoO_2, MCNs-MoS_2, MCNs-MoN_2 and MCNs-MoP configuration at 0.1-0.5 mV s^{-1}.

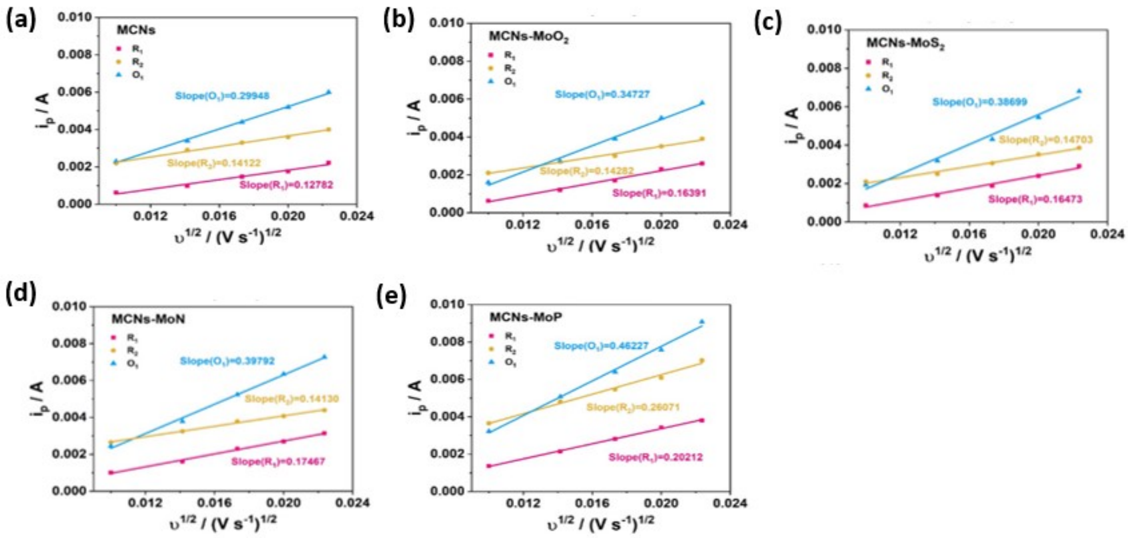

Fig. S12. (a-e) The corresponding linear plot of peak current.

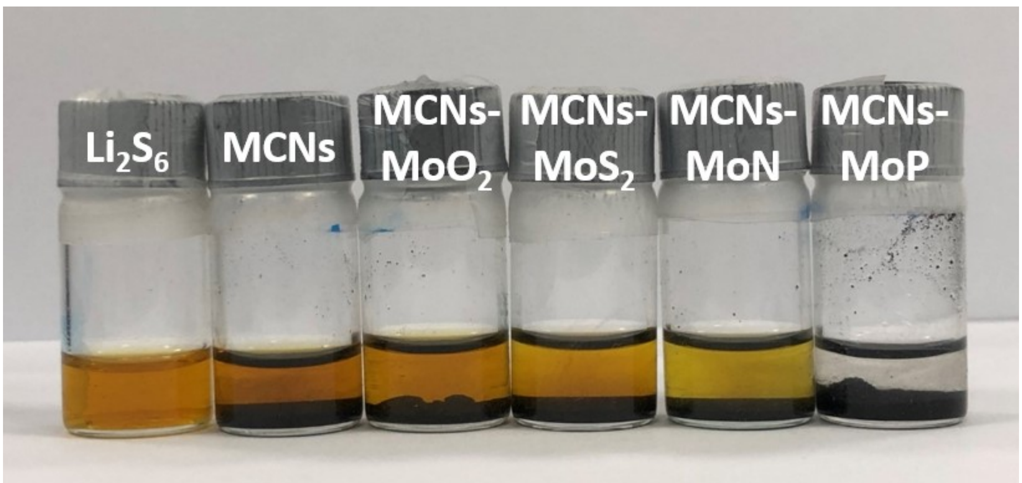

Fig. S13 The photograph of Li_2S_6 solution after contact with MCNs, MCNs-MoO_2, MCNs-MoS_2, MCNs-MoN, and MCNs-MoP for 12h.

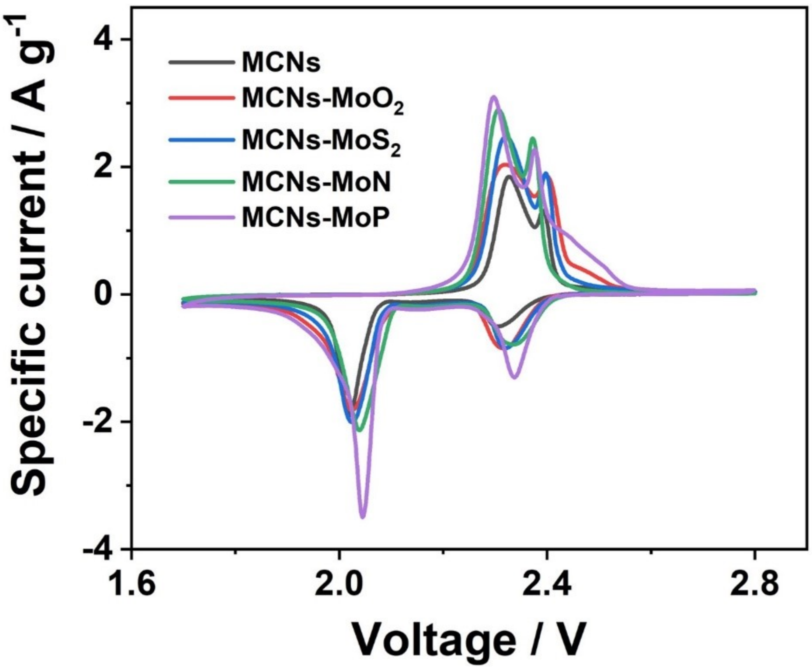

Fig. S14. The CV curves of MCNs, MCNs-MoO_2, MCNs-MoS_2, MCNs-MoN_2 and MCNs-MoP cells within the voltage window of 1.7-2.8 V at the scan rate of 0.1 mV s^{-1}.

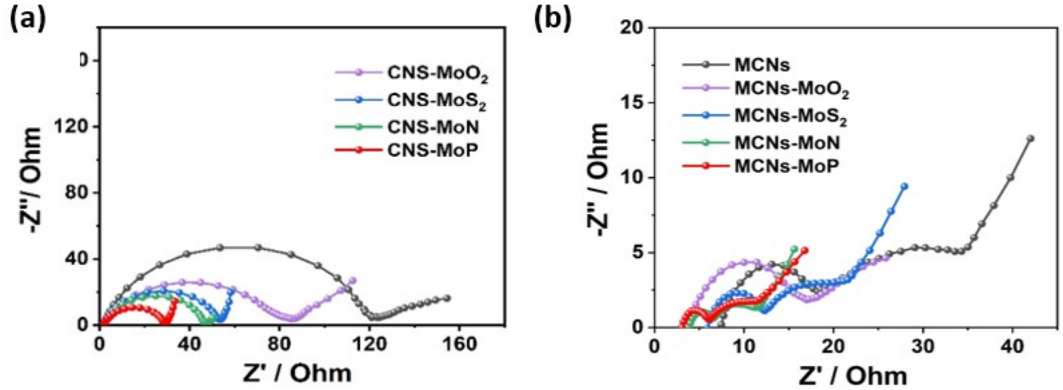

Fig. S15. EIS spectra of cells with different separators before (a) and after 100 cycling (b).

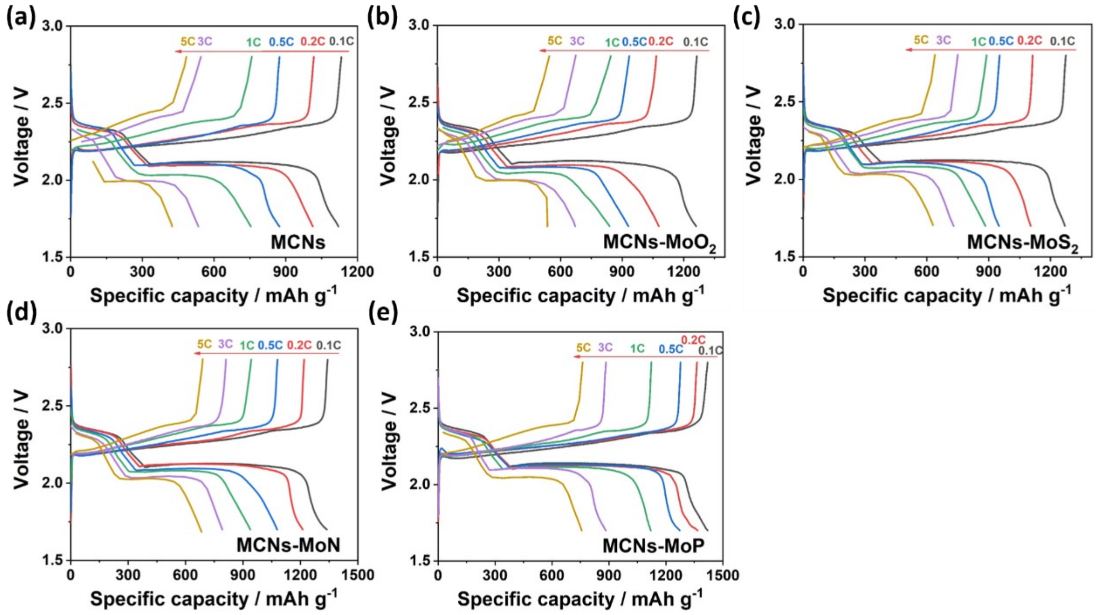

Fig. S16. The galvanostatic discharge/charge profiles of the electrodes at different rates. **(a-e)** The discharge/charge profiles of MCNs, MCNs-MoO_2, MCNs-MoS_2, MCNs-MoN_2 and MCNs-MoP cells at the rates varying from 0.1 to 5 C, respectively.

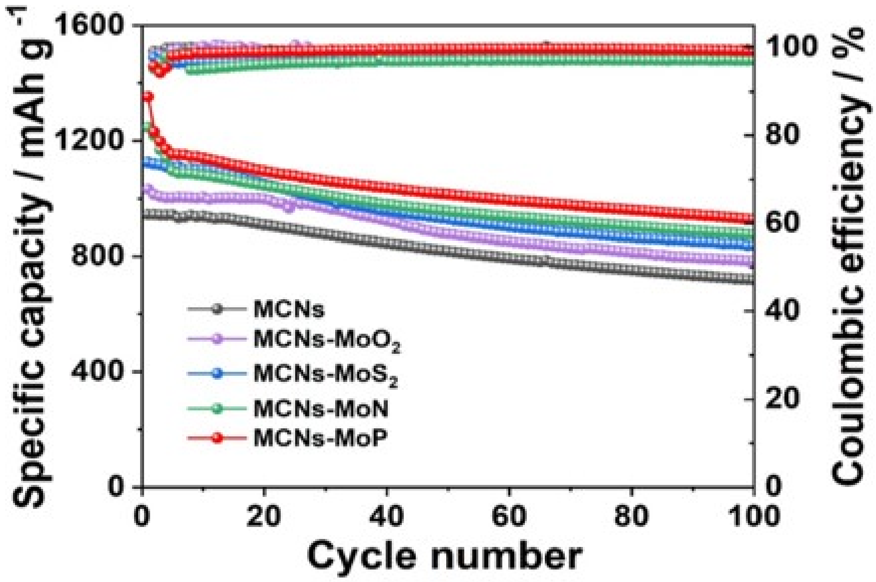

Fig. S17. Coulombic efficiency and cycling performance of all separators at 0.2 C.

Table S1. Summary of Li^+ diffusion coefficients (D_{Li^+}) for different separators

Sample	D_{Li^+} at peak R_1 [$cm^2\ s^{-1}$]	D_{Li^+} at peak R_2 [$cm^2\ s^{-1}$]	D_{Li^+} at peak O_1 [$cm^2\ s^{-1}$]
MCNs	$2.94*10^{-9}$	$9.77*10^{-9}$	$2.13\ *10^{-8}$
MCNs-MoO_2	$5.2*10^{-9}$	$1.03*10^{-8}$	$2.21*10^{-8}$
MCNs-MoS_2	$5.46*10^{-9}$	$1.08*10^{-8}$	$2.91*10^{-8}$
MCNs-MoN	$5.89*10^{-9}$	$1.13*10^{-8}$	$3.26*10^{-8}$
MCNs-MoP	$8.86*10^{-9}$	$3.00*10^{-8}$	$5.06*10^{-8}$

Table S2. Comparison of electrochemical performance of this work with previous excellent works involving MCNs-MoP separators using carbon-sulfur cathodes in Li-S batteries.

Separator	Initial capacity mAh g^{-1}	Capacity retention mAh g^{-1}	Cycles	Fading rate per cycle %	Rate capacity mAh g^{-1}	Sulfur Loading mg cm^{-2}	Ref.
MoO_3@CNT	~1200 (1 C)	641	400	0.11	655 (3 C)	1.0	(1)
MoO_3	1377 (0.5 C)	684	200	0.25	1074 (1 C)	0.9-1.0	(2)
MoS_2/Celgard	808 (0.5 C)	401	600	0.083	550 (1 C)	/	(3)
LDH@NG	812 (2 C)	337	999	0.06	709 (2 C)	1.2	(4)
MoN-G	1061 (0.5 C)	678	500	0.072	606 (2 C)	~0.8 (Li_2S)	(5)
Edg-MoS_2/C	935 (1C)	494	1000	0.047	602 (5 C)	1.7	(6)
Co_9S_8-Celgard	1385 (0.1 C)	1190	200	0.070	428 (2 C)	2	(7)
N,S-Mo_2C/C-	~1000	524	600	0.08	630	0.9-1.3	(8)

ACF	(1C)				(5 C)		
KB/Mo_2C	813 (1C)	439	600	0.076	437 (3.5 C)	1.2	(9)
CoS_2/NSCNHF@C-200	960.9 (0.5C)	661.3	100	0.312	532.1 (2 C)	2	(10)
CuNWs-GN/PI/LLZO	~1200 (0.5A g^{-1})	~500	300	0.194	488.3 (2A g^{-1})	3	(11)
MCNs-MoP	**1218.0 (0.5C)**	**640.8**	**500**	**0.09%**	**756.7 (5C)**	**1.3-1.5**	**This work**

Table S3. Comparison of the low-temperature performance of Li-S batteries with representative work.

Separator	Cathode	Temperature °C	Rate performance mAh g^{-1}		Cycle Performance mAh g^{-1}	Ref
			1C	2C		
PP	rGO-$MoSe_2$	0 -25	779 272		538 (500th, 0.5C) 253 (500th, 0.5C)	(12)
Ni3Fe@HPC-CNT	Pure S	0 -10 -25	1166 920 294	1038 420 225	476 (400th, 0.5C)	(13)
PP	Ni@C/ graphene	-40 -50	/	/	354 (200th, 0.1C) 274 (400th, 0.1C)	(14)
AAPP/CB@PP@LAGP	70% S/CB	0 -20	/	/	800.7 (100th, 0.5C) 372.2 (100th, 0.5C)	(15)
MCNs-MoP	**80%S/ Super C**	**-40**			**350.2(100th, 0.1C)**	**This work**

References

1 L.Y. Luo, X.Y. Qin, J.X. Wu, G.M. Liang, Q. Li, M. Liu, B.H. Li, An interwoven MoO_3@ CNT Scaffold Interlayer for High-Performance Lithium-Sulfur Batteries. J. Mater. Chem. A. 2018, 6, 8612-8619.

2 S. Imtiaz, Z.A. Zafar, R. Razaq, D. Sun, Y. Xin, Q. Li, Z.L. Zhang, L. Zheng, Y.H. Huang, J.A. Anderson, Electrocatalysis on Separator Modified by Molybdenum Trioxide Nanobelts for Lithium-Sulfur Batteries. Adv. Mater. Interfaces. 2018, 5, 1800243.

3 Z.A. Ghazi, X. He, A.M. Khattak, N.A. Khan, B. Liang, A. Iqbal, J.X. Wang, H. Sin, L.S. Li, Z.Y. Tang, MoS_2/Celgard Separator as Efficient Polysulfide Barrier for Long-Life Lithium-Sulfur Batteries. Adv. Mater. 2017, 29, 1606817.

4 H.J. Peng, Z.W. Zhang, J.Q. Huang, G. Zhang, J. Xie, W.T. Xu, J.L. Shi, X. Chen, X.B. Cheng, Q. Zhang, A Cooperative Interface for Highly Efficient Lithium-Sulfur Batteries, Adv. Mater. 2016, 28, 9551-9558.

5 D. Tian, X.Q. Song, M.X. Wang, X. Wu, Y. Qiu, B. Guan, X.Z. Xu, L.S. Fan, N,Q. Zhang, K.N. Sun, MoN Supported on Graphene as a Bifunctional Interlayer for Advanced Li-S Batteries. Adv. Energy Mater. 2019, 9, 1901940.

6 N. Zheng, G.Y. Jiang, X. Chen, J.Y. Mao, N. Jiang, Y.S. Li, Battery Separators Functionalized with Edge-Rich MoS_2/C Hollow Microspheres for the Uniform Deposition of Li_2S in High-Performance Lithium-Sulfur Batteries. Nano-Micro Lett. 2019, 11, 43.

7 J.R. He, Y.F. Chen, A. Manthiram, Vertical Co_9S_8 Hollow Nanowall Arrays Grown on a Celgard Separator as a Multifunctional Polysulfide Barrier for High-Performance Li-S Batteries. Energy Environ. Sci. 2018, 11, 2560-2568.

8 H.T. Li, Q. Jin, D.M. Li, X.H. Huan, Y.M. Liu, G.L. Feng, J. Zhao, W. Yang, Z.G. Wu, B.H. Zhong, X.D. Guo, B. Wang, Mo_2C-Embedded Carambola-like N,S-Rich Carbon Framework as the Interlayer Material for High-Rate Lithium-Sulfur Batteries in a Wide Temperature Range. ACS Appl. Mater. Interfaces. 2020, 12, 22971-22980

9 M.X. He, X. Li, W.H. Li, M. Zheng, J.J. Wang, S.B. Ma, Y.L. Ma, G.P. Yin, P.J. Zuo, X.L. Sun, Immobilization and Kinetic Promotion of Polysulfides by Molybdenum Carbide in Lithium-Sulfur Batteries. Chem. Engineering J. 2021, 411, 128563.

10 J.L. Wang, W. Cai, X.W. Mu, L.F. Han, N. Wu, C. Liao, Y.C. Kan, Y. Hu, Designing of Multifunctional and Flame Retardant Separator towards Safer High-Performance Lithium-Sulfur Batteries. Nano Res. 2021, 14, 4865-4877

11 Z.F. Zhou, B.B. Chen, T.T. Fang, Y. Li, Z.F. Zhou, Q.J. Wang, J.J. Zhang, Y.F. Zhao, A Multifunctional Separator Enables Safe and Durable Lithium/Magnesium-Sulfur Batteries under Elevated Temperature. Adv. Energy Mater. 2020, 10, 1902023

12 C.Y. Fan, Y.P. Zheng, X.H. Zhang, Y.H. Shi, S.Y. Liu, H.C. Wang, X.L. Wu, H.Z. Sun, J.P. Zhang, High-Performance and Low-Temperature Lithium-Sulfur Batteries: Synergism of Thermodynamic and Kinetic Regulation. Adv. Energy Mater. 2018, 8, 1703638

13 P. Zeng, C. Liu, C. Cheng, C. Yuan, K. Dai, J. Mao, L.R. Zheng, J. Zhang, L.Y. Chang, S.C. Haw, T.S. Chan, H.P. Lin, L. Zhang, Propelling Polysulfide Redox Conversion by d-Band Modulation for High Sulfur Loading and Low Temperature Lithium-Sulfur Batteries. J. Mater. Chem. A. 2021, 9, 18526-18536

14 Z. Yu, B.L. Wang, X.B. Liao, K.N. Zhao, Z.F. Yang, F.J. Xia, C.L. Sun, Z. Wang, C.Y. Fan, J.P. Zhang, Y.G. Wang, Boosting Polysulfide Redox Kinetics by Graphene-Supported Ni Nanoparticles with Carbon Coating. Adv. Energy Mater. 2020, 10, 2000907

15 C. Ma, Y.M. Feng, X.J. Liu, Y. Yang, L.J. Zhou, L.B. Chen, C.L. Yan, W.F. Wei, Dual-Engineered Separator for Highly Robust, All-Climate Lithium-Sulfur Batteries. Energy Storage Mater. 2020, 32, 46-54.